Future Circular Collider

PUBLICATION

Length optimization of the detector region dipoles in LHeC and FCC-eh

Martin, Roman (CERN) *et al.*

02 November 2018

The European Circular Energy-Frontier Collider Study (EuroCirCol) project has received funding from the European Union's Horizon 2020 research and innovation programme under grant No 654305. The information herein only reflects the views of its authors and the European Commission is not responsible for any use that may be made of the information.

The research leading to this document is part of the Future Circular Collider Study

The electronic version of this FCC Publication is available on the CERN Document Server at the following URL :
<http://cds.cern.ch/record/2644892

25 October 2018
roman.martin@cern.ch

Length optimization of the detector region dipoles in LHeC and FCC-eh

Roman Martin, Rogelio Tomás
CERN, CH-1211 Geneva, Switzerland

Keywords: LHeC, FCC-eh, detector dipole, synchrotron radiation

Summary

In the LHeC and FCC-eh interaction region designs strong quadrupole septa are used to focus the colliding proton beam at the interaction point. Since the electron beam has a significantly lower beam rigidity it must pass through these magnets' field free region. This leads to a large angle between the two incoming colliding beams. Dipoles around the Interaction Point (IP) bend the electron beam into head-on collisions with the proton beam and separate the two beams after the IP. Although these dipoles are weak, the high electron beam energy and current lead to a synchrotron radiation power in the range of tens of kW in the immediate vicinity of the detector. This note shows that there is an optimum dipole length that minimizes the synchrotron radiation power for a given distance L^* between IP and the first quadrupole. This optimum dipole length is shown to be $\frac{2}{3}L^*$.

Contents

1 Interaction region layout of LHeC and FCC-eh

The Interaction Region (IR) layout of LHeC [1] is shown in Fig. (1). The colliding proton beam (p2, red) is strongly focused by the quadrupole septa Q1-Q3 while the non-colliding proton beam (p1, blue) and the electron beam (black) pass through the field free regions of the septa. The first detector region dipole (not depicted) bends the electron beam into head-on collisions with p2, a second dipole with opposite polarity separates the two beams after the collision. The two dipoles have a field of 0.3 T, corresponding to an integrated field of 2.7 Tm each, and thus do not disturb the 7 TeV proton beams noticeably. FCC-eh will use a similar IR design with L^* and magnet lengths scaled to account for the higher proton beam energy. Due to the high energy and current of the electron beam a synchrotron radiation fan of almost 50 kW is emitted in the detector region. This radiation must be extracted without damage to or significant heat load on the superconducting magnets, while keeping the background in the detector, e.g. due to backscattered photons, to a minimum. Any reduction in the radiated power will ease this task.

In the LHeC design report the dipoles were chosen as long a possible to reduce the critical energy and power. However, since the purpose of the dipole is to create a horizontal separation between two beams, a solution with a lower synchrotron radiation power can be constructed. The approach is to make use of a short drift after the dipole to increase the separation between the two diverging beams without additional synchrotron radiation.

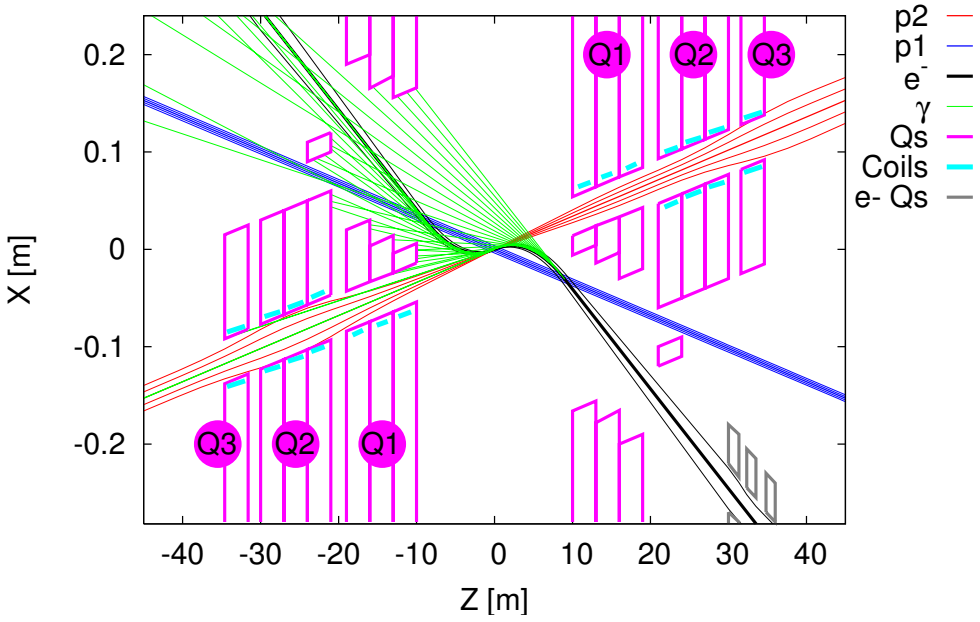

Figure 1: Layout of the LHeC interaction region as shown in the Conceptual Design Report [1]. The bending dipoles for the electron beam are not depicted but extend from $z = -9$ m to $z = +9$ m, covering almost the whole of L^*.

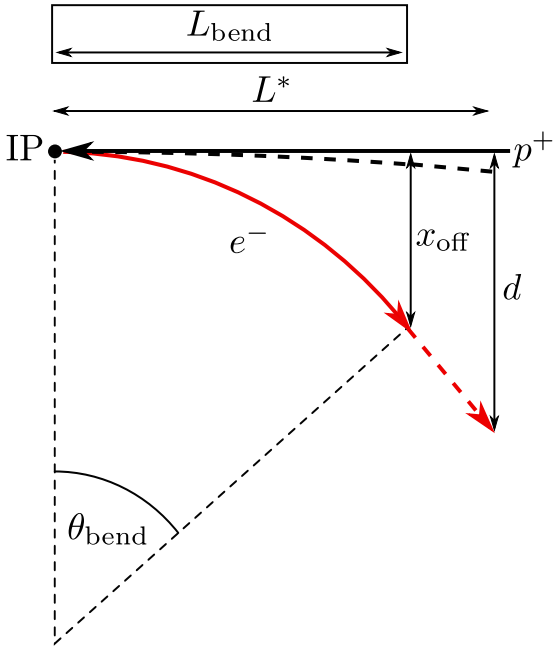

Figure 2: Geometry of the problem: electrons (e^-) are bend downwards by the dipole field while the proton (p^+) beam is almost undisturbed.

2 Optimum length of the detector region dipoles

In order to provide enough separation at the first final focus quadrupole, the dipole needs to separate the proton and electron beams. Figure 2 illustrates the geometry of the problem. The offset of the electron beam from the almost straight proton beam orbit can be described by

$$x_{\text{off}} = (1 - \cos\theta_{\text{bend}})\,\rho_e = (1 - \cos\theta_{\text{bend}})\,\frac{L_{\text{bend}}}{\theta_{\text{bend}}}\,, \tag{1}$$

with $\rho_e = \frac{L_{\text{bend}}}{\theta_{\text{bend}}}$ the bending radius of the electron beam. The Taylor expansion of Eq. (1) in θ_{bend} to the second order yields

$$x_{\text{off}} \approx \frac{L_{\text{bend}}\theta_{\text{bend}}}{2} + \mathcal{O}(\theta_{\text{bend}}^3)\,. \tag{2}$$

The electron beam trajectory has a slope of

$$x'_{\text{off}} \approx \theta_{\text{bend}}\,. \tag{3}$$

at the end of the bend. Consequently, the beam offset at the entrance of the final focus system is

$$\begin{aligned} d &= x_{\text{off}} + x'_{\text{off}}(L^* - L_{\text{bend}}) && (4)\\ &\approx \frac{L_{\text{bend}}\theta_{\text{bend}}}{2} + \theta_{\text{bend}}(L^* - L_{\text{bend}}) \\ &\approx \theta_{\text{bend}}\left(L^* - \frac{L_{\text{bend}}}{2}\right)\,, && (5) \end{aligned}$$

where the minimum separation $d = d_{\text{min}}$ is given by the magnet design. Consequently

$$\theta_{\text{bend}} = \frac{d_{\text{min}}}{L^* - \frac{L_{\text{bend}}}{2}} \tag{6}$$

To account for the fact that the proton beam is slightly bent in the dipole as well, the right hand side of Eq. (4) can simply be multiplied by

$$1 - \frac{P_e}{P_p} \tag{7}$$

as the offset of the bent proton beam (dashed black line in Fig. 2) is approximately $\frac{P_e}{P_p}$ times the offset of the electron beam. For LHeC and FCC-eh this is a correction on the permille level and is ignored here.

In [2] the synchrotron radiation power radiated in the dipole on one side of the IP is calculated as

$$P_{\text{SR}}[\text{MW}] = 8.86 \times 10^{-2} \frac{E^4[\text{GeV}]\theta_{\text{bend}}}{2\pi\rho_e} I \ . \tag{8}$$

In terms of dipole parameters, this can be reduced to

$$P_{\text{SR}} \propto \frac{\theta_{\text{bend}}}{\rho_e} \tag{9}$$

and since $\rho_e \approx \frac{L_{\text{bend}}}{\theta_{\text{bend}}}$ the synchrotron radiation power is proportional to

$$P_{\text{SR}} \propto \frac{\theta_{\text{bend}}^2}{L_{\text{bend}}} = \frac{d_{\text{min}}^2}{\left(L^* - \frac{L_{\text{bend}}}{2}\right)^2 L_{\text{bend}}} \ . \tag{10}$$

Figure 3 shows this dependency of P_{SR} for arbitrary d_{min} and L^* in the relevant region of $0 < L_{\text{bend}} \leq L^*$. It is immediately clear that $L_{\text{bend}} = L^*$ does not provide the lowest synchrotron radiation power. From Eq. (10) we can get the optimum L_{bend} by searching for zeros of the derivative

$$\frac{\partial P_{\text{SR}}}{\partial L_{\text{bend}}} \propto -\frac{d_{\text{min}}^2 \left(L^* - \frac{3}{2} L_{\text{bend}}\right)}{L_{\text{bend}}^2 \left(L^* - \frac{L_{\text{bend}}}{2}\right)^3} \ , \tag{11}$$

obtaining

$$\boxed{L_{\text{bend}} = \frac{2}{3} L^* \ ,} \tag{12}$$

so this is the optimum length for the dipole magnet.

3 Synchrotron radiation power vs. critical energy

It is further interesting to compare the decrease in synchrotron power with the optimum length compared to the maximum possible length $L_{\text{bend}} = L^*$ assumed in previous studies [1, 2]. In order to simply get a ratio, Eq. (10) can be used. By inserting $L_{\text{bend}} = L^*$, we get that

$$P_{\text{SR, long}} \propto 4 \frac{d_{\text{min}}^2}{L^{*3}} \tag{13}$$

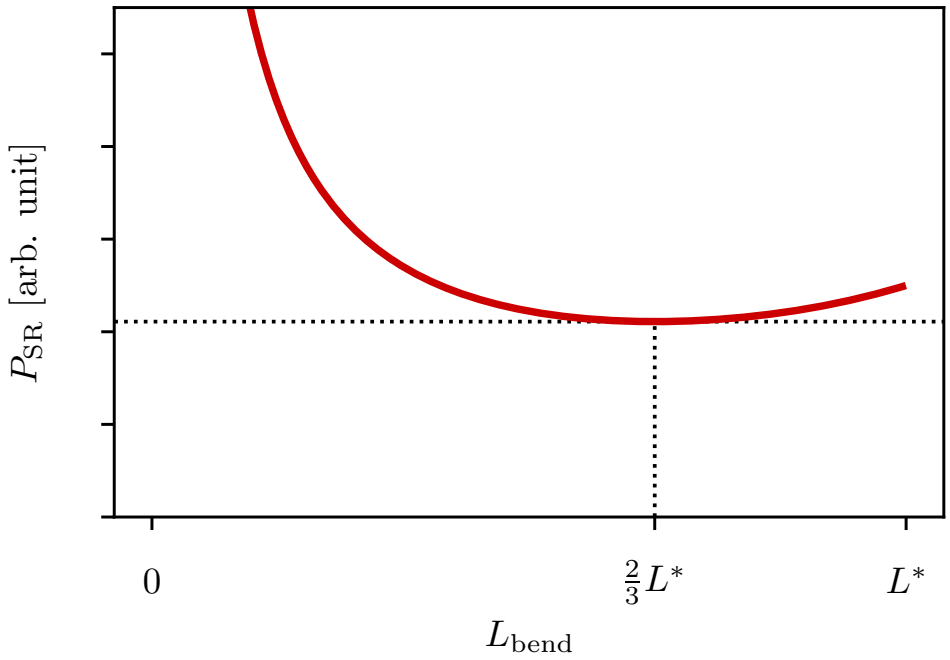

Figure 3: Synchrotron radiation power as a function of L_{bend} for an arbitrary set of parameters. It is evident that the radiated power is not minimal for $L_{\mathrm{bend}} = L^*$.

while the optimized length $L_{\mathrm{bend}} = \frac{2}{3}L^*$ only yields

$$P_{\mathrm{SR,\,opt}} \propto \frac{27}{8}\frac{d_{\mathrm{min}}^2}{L^{*3}} \tag{14}$$

The ratio is

$$\boxed{\frac{P_{\mathrm{SR,\,opt}}}{P_{\mathrm{SR,\,long}}} = 0.844} \tag{15}$$

so the optimized dipole length results in a $\underline{15.6\,\%}$ lower synchrotron radiation power. The stronger bending that is necessary for the shorter dipole also guarantees that the normalized separation of the two beams at the first long range beam-beam encounter is larger than in the long dipole option. However, it also means the critical energy of the synchrotron radiation increases. The critical energy is given by

$$E_{\mathrm{crit}} = \frac{3\hbar c}{2\rho_e}\gamma^3 \propto \frac{1}{\rho_e} = \frac{\theta_{\mathrm{bend}}}{L_{\mathrm{bend}}}. \tag{16}$$

Using Eq. (6) again, we can deduce that

$$E_{\mathrm{crit}} \propto \frac{d_{\mathrm{min}}}{\left(L^* - \frac{L_{\mathrm{bend}}}{2}\right) L_{\mathrm{bend}}}. \tag{17}$$

Inserting both options for L_{bend} results in

$$L_{\text{bend}} = L^* \qquad \rightarrow \qquad E_{\text{crit, long}} \propto 2\frac{d_{\text{min}}}{L^{*2}} \tag{18}$$

$$L_{\text{bend}} = \frac{2}{3}L^* \qquad \rightarrow \qquad E_{\text{crit, opt}} \propto \frac{9}{4}\frac{d_{\text{min}}}{L^{*2}} \tag{19}$$

resulting in the ratio

$$\boxed{\frac{E_{\text{crit, opt}}}{E_{\text{crit, long}}} = \frac{9}{8} = 1.125} \tag{20}$$

so the critical energy of the optimized dipole increases by 12.5 %.

Aside from the optimum L^*, Eq. (10) offers another insight: While the synchrotron radiation power is proportional to d_{min}^2, and thus the magnet design should keep d_{min} as low as possible, it is also proportional to $L^{*^{-3}}$ (as L_{bend} can be expressed in terms of L^*). Consequently, the choice of L^* provides a strong leverage to reduce the synchrotron radiation power, however, the usual drawbacks of a long L^* like aperture need in the quadrupoles still have to be taken into account.

References

[1] LHeC Study Group. A large hadron electron collider at cern report on the physics and design concepts for machine and detector. *Journal of Physics G: Nuclear and Particle Physics*, **39**(7):075001, 2012.

[2] E. Cruz-Alaniz, D. Newton, R. Tomás, and M. Korostelev. Design of the large hadron electron collider interaction region. *Phys. Rev. ST Accel. Beams*, **18**:111001, Nov 2015.